GaAs, AlGaAs, and InGaAs epilayers containing As clusters: semimetal/semiconductor composites

M. R. Melloch[a], J. M. Woodall[b], N. Otsuka[a], K. Mahalingam[a], C. L. Chang[a] and D. D. Nolte[a]
[a]*Purdue University, West Lafayette, IN (USA)*
[b]*IBM T. J. Watson Research Center, Yorktown Heights, NY (USA)*

Abstract

A new kind of semiconductor composite material is demonstrated with a dispersion of semimetallic particles with properties common to high-quality single crystals. These materials are arsenides such as GaAs, AlGaAs, and InGaAs containing arsenic clusters. These composites are formed by incorporating excess As in the semiconductor, which precipitate with anneal. The incorporation of the excess As is accomplished by molecular beam epitaxy at low substrate temperatures. We demonstrate that the cluster densities can be controlled with the coarsening anneal. Furthermore, we demonstrate that heterojunctions and doping can be used to control the positioning of the As clusters.

1. Introduction

Everyone is well aware of the virtues of composite materials. However, with some exceptions, these virtues are usually only associated with those properties useful for mechanical applications. Attempts to engineer new and useful electronic and photonic properties in semiconductor materials through metal/semiconductor composites has met with limited success. The reason is simple: useful crystalline devices usually require semiconductors with relatively low defect densities, while most compositing techniques render semiconductors highly defective. Recently, we have demonstrated a new kind of semiconductor composite material with a dispersion of semimetallic particles with some properties common to good quality single crystals. These materials are arsenides, such as GaAs, AlGaAs and InGaAs, containing arsenic clusters, which we designate as GaAs:As [1], AlGaAs:As [2] or InGaAs:As [3].

These semimetal/semiconductor composites exhibit several interesting properties. The As clusters act as internal Schottky barriers, and therefore the depletion regions surrounding the As clusters compensate for p- and n-dopants in GaAs:As and AlGaAs:As [4]. This is the reason that GaAs:As is so effective in eliminating sidegating when used as a buffer layer below field-effect transistors [5–7]. In addition, layers that are grown at normal substrate temperatures on top of GaAs:As exhibit extremely high electrical quality [7]. The As clusters should be very efficient recombination centres, and in conjunction with other defects in the film make GaAs:As a very fast photoconductor. Several pulse generation systems have been demonstrated using GaAs:As as a photoconducting switch [8–10]. GaAs:As responds to light below the bandgap of GaAs due to internal photoemission from the As clusters [11, 12]. This internal photoemission has been used to make a 1.3 μm GaAs PiN photodetector [13]. Recently we have observed a large room temperature electro-optic effect in GaAs:As and AlGaAs:As; almost a 60% differential transmission has been obtained for a 1 μm thick $Al_{0.25}Ga_{0.75}As$:As epilayer [14, 15]. Using this electro-optic effect, along with charge storage on As clusters, we have demonstrated holographic storage in AlGaAs:As [16].

2. Composite formation

The starting point for forming these composite materials is to incorporate excess As into the epilayers. This is accomplished using molecular beam epitaxy (MBE) with typical group III and As fluxes, but at a reduced substrate temperature, typically in the range of 200 to 300 °C. This results in an incorporation of as much as 2% excess As in the epilayer in the form of point defects, and an expansive lattice strain of approximately 0.1% [17, 18]. Owing to this strain there is a critical thickness beyond which there is a breakdown in the crystallinity of the growing film, this critical thickness being a function of the amount of excess As incorporated [19]. The dimer As_2 or the tetramer As_4 can be used as the arsenic flux [20, 21]. Upon annealing this

0921-5107/93/$6.00

material the excess As precipitates, forming a high-quality III–V matrix containing As clusters [1], with a corresponding order of magnitude reduction in the lattice strain. It has been observed that even though a considerable amount of the excess As has precipitated, there are still in the neighbourhood of 10^{18} cm^{-3} As antisites after an anneal of 600 °C for 10 min [22, 23]. Therefore our typical precipitation anneals are in the range of 700 to 950 °C.

The total energy of these two-phase systems is reduced by an increase in size and hence decrease in density of the clusters due to a reduction in total precipitate-to-matrix interfacial area [15, 24]. Therefore the final average cluster size and corresponding density is controlled by the temperature and duration of the coarsening anneal, while the amount of excess As in the epilayer is controlled by the substrate temperature during MBE. This is illustrated in Fig. 1, where the average As cluster size and density are plotted as a function of coarsening anneal temperature for a GaAs sample that contained 0.9% excess As. The data in Fig. 1 were determined using transmission electron microscopy (TEM). It is clear from Fig. 1 that the control of the density with the coarsening anneal is routine. For a given density of As clusters the average size of the As clusters is determined by the excess As in the film. Therefore complete control of both the density and average size of the clusters requires setting the excess As in the starting epilayer by use of the substrate temperature during MBE [2] followed by the coarsening anneal. Arsenic clusters have been observed in GaAs [1], AlGaAs [2] and InGaAs [3, 25] after this technique of low-temperature MBE followed by an anneal.

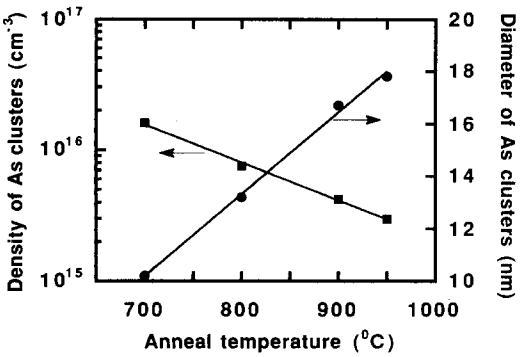

Fig. 1. Arsenic cluster density and average diameter as a function of anneal temperature for isochronal anneals of 30 s with a GaAs sample containing 0.9% excess As.

The As clusters act as internal Schottky barriers, and hence there will be a depletion region surrounding each cluster. In n- or p-doped material, if these depletion regions overlap, the material will be highly resistive. We have seen that the density and hence spacing between As clusters can be controlled with the coarsening anneal. Therefore, by annealing doped material, the clusters will eventually be spaced far enough apart that the depletion regions can be accommodated, leaving conducting regions between clusters [26]. This is illustrated in Table 1 for samples from a GaAs epilayer that contained 1.5% excess As and were doped n-type at 5×10^{18} cm^{-3}. (Note that as-grown all the Si atoms will be on Ga sites [27].) In Table 1, the 600 °C anneal was for 1 h and the higher temperature anneals were for 30 s. On a sample at each anneal, a Hall bar was fabricated to ascertain the density and mobility of the carriers, and TEM imaging was used to obtain cluster average size and density information. As can be seen in Table 1, the material begins to exhibit n-type conductivity as the depletion regions no longer overlap. For the sample annealed at 900 °C for 30 s, a carrier density of 1×10^{18} cm^{-3} and mobility of 1320 cm^2 V^{-1} s^{-1} were measured. This mobility is comparable to that obtained for high-quality highly stoichiometric GaAs doped at 1×10^{18} cm^{-3}.

3. Cluster formation at heterojunctions

Arsenic clusters can be readily formed in GaAs and AlGaAs. If a GaAs/AlGaAs heterojunction is present during cluster coarsening there will be a preferential

TABLE 1. Effect of annealing on As cluster coarsening, carrier mobility and density for a sample doped n-type with silicon at 5×10^{18} cm^{-3}. The 600 °C anneal was for 1 h, all other anneals were for 30 s

Anneal temperature (°C)	Average cluster diameter (Å)	Average inter-cluster spacing (Å)	Cluster density ($\times 10^{16}$ cm^{-3})	Cluster volume fraction	Electron density ($\times 10^{18}$ cm^{-3})	Mobility (cm^2 V^{-1} s^{-1})
600	55	180	17	0.015	—	—
700	70	225	8.7	0.015	0.12	680
800	150	475	0.93	0.016	0.75	1180
900	200	675	0.325	0.013	1.1	1320

coarsening of the clusters to the lower bandgap GaAs regions [24, 28, 29]. This is due to the differences in interfacial energy between the As cluster and semiconductor matrices. (An As cluster in GaAs has a lower interfacial energy than an As cluster in AlGaAs, since the Ga–As bond is weaker than the Al–As bond.) Therefore at a GaAs/AlGaAs heterojunction, there is a preferential growth of the clusters on the GaAs side during cluster coarsening. This is illustrated in Figs. 2(a) and 2(b) for a sample consisting of 10 nm GaAs layers surrounded by 100 nm AlGaAs layers after anneals at 700 °C for 5 min (Fig. 2(a)) and 700 °C for 1.5 h (Fig. 2(b)). We know that after MBE of the structure in Fig. 2 there is approximately the same amount of excess As in the 10 nm GaAs and 100 nm AlGaAs layers [2]. After the 700 °C anneal for 5 min (Fig. 2(a)), enough coarsening has occurred to give a much higher density of clusters in the 10 nm GaAs layers than in the 100 nm AlGaAs regions. With further coarsening, as occurs during the 700 °C anneal for 1.5 h (Fig. 2(b)), there is further transfer of the excess As from the AlGaAs regions to the GaAs regions.

It is also possible to form GaAs wells that are free of As clusters but that have clusters in the surrounding AlGaAs layers [30]. The two keys to accomplish this reversal in positioning of the As clusters are first to grow a film where there is excess As in the AlGaAs regions but no excess As in the GaAs wells, and second to place an As diffusion barrier between the GaAs and AlGaAs regions. The first task is accomplished by growing the GaAs regions using migration-enhanced epitaxy (MEE), which results in highly stoichiometric GaAs even at low substrate temperatures [31], and growing the AlGaAs using MBE at low substrate temperatures to incorporate 1–2% excess As. The second task is accomplished by placing thin AlAs layers between the AlGaAs and GaAs regions, which act as As diffusion barriers [32]. The results of this technique are illustrated in Fig. 3. The white lines in Fig. 3 are the AlAs layers, of which only the lower AlAs layer is indicated. Clearly seen in Fig. 3 is a high concentration of As clusters (about 9) in the AlGaAs regions with very few As clusters (1 or 2) in the GaAs regions and none in the AlAs layers. Note that the clusters in the lower thick GaAs region, which was grown by MBE and hence has excess As as-grown, are much larger in diameter than the clusters in the AlGaAs layers, due to the AlAs layers constraining the size of the clusters in the AlGaAs layers.

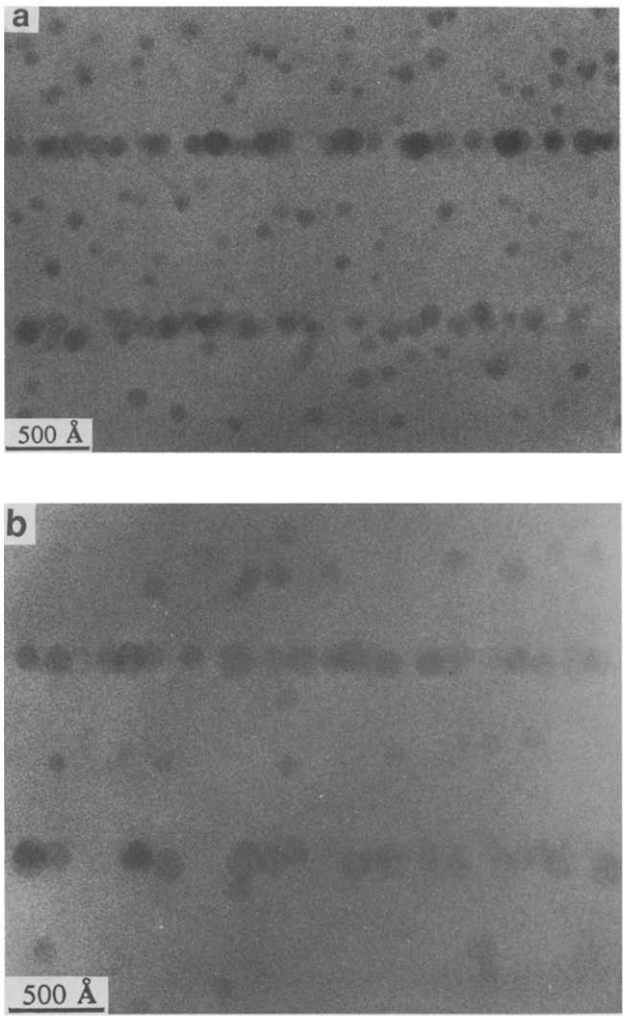

Fig. 2. Arsenic clusters in a structure consisting of 10 nm GaAs layers surrounded by 100 nm AlGaAs layers after anneals of (a) 700 °C for 5 min and (b) 700 °C for 1.5 h.

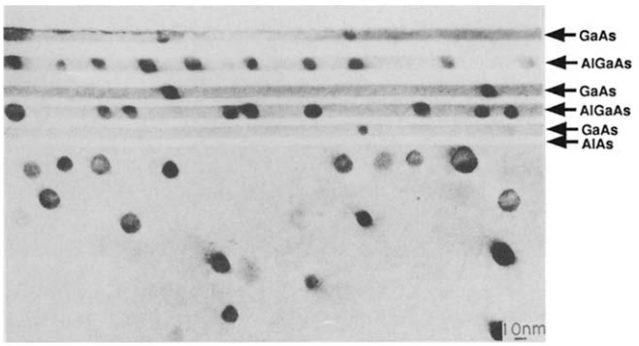

Fig. 3. TEM image of a film structure grown at 260 °C using As_4 and annealed for 30 s at 700 °C. The white lines are AlAs layers (the lowest one is marked) and were either 6 nm or 12 nm thick. The region below the marked AlAs layer is a GaAs temperature transition region. The three GaAs wells in the image are indicated with arrows. The AlAs layers and the GaAs regions between the AlAs layers were grown by MEE and as-grown are highly stoichiometric. The $Al_{0.2}Ga_{0.8}As$ layers and the GaAs temperature transition layer were grown by MBE and as-grown have a large excess of As.

4. Controlling cluster formation with doping

During annealing, some very interesting phenomena are observed if the layers are doped, owing to the fact that the As clusters act as Schottky barriers and hence are charged [33–35]. This is illustrated in Figs. 4, 5(a) and 5(b). Figure 4 is a transmission electron micrograph of a sample that was grown at 250 °C and annealed for 30 s at 800 °C. In Fig. 4, the white lines are 5 nm AlAs layers that serve as markers for the TEM imaging; the other regions are GaAs. There are four GaAs regions of interest in Fig. 4. The first GaAs region, in the lower part of the figure between the lower two AlAs markers, contains a growth interruption of 3 min duration. The growth interruption was accomplished by closing the shutter to the Ga effusion cell while maintaining the As flux. In Fig. 4 the growth interruption is seen to have no effect on the As cluster formation. The next GaAs region contained three planes of Si atoms, an n-type dopant, every 100 nm. These planes were formed by closing the shutter in front of the Ga effusion cell while maintaining the As flux, opening the Si effusion cell for 3 min to deposit 5×10^{12} cm^{-2} Si atoms, then resuming the Ga flux. In Fig. 4, the As clusters are seen to coarsen preferentially on these planes of Si atoms. The next GaAs region contained three planes of 5×10^{12} cm^{-2} Be atoms, a p-type dopant, using the same procedure as just described. In Fig. 4, the As clusters are seen to coarsen preferentially between the planes of Be atoms. Finally, the last GaAs region, which has an AlAs marker only on the bottom, contained a plane of In atoms, an isoelectronic site in GaAs. In Fig. 4, the plane of In atoms is seen to have no affect on the As cluster coarsening, although the amount of excess As in this region is lower than in others, probably due to As escaping from the surface during the anneal.

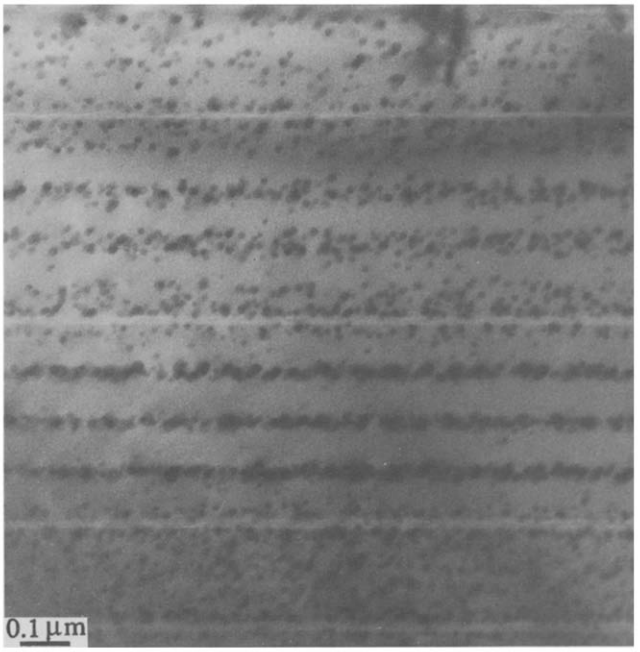

Fig. 4. TEM image of a film structure grown at 250 °C using As_2 and annealed for 30 s at 800 °C. The white lines are 5 nm AlAs layers. Between the lower two AlAs layers is a 200 nm GaAs region that contained a 3 min growth interruption in the centre. There is no apparent effect on the As cluster coarsening due to the growth interruption. The next 400 nm region is a GaAs layer that contained three planes of Si dopants. The As clusters are lined up on the planes of Si dopants. The next 400 nm region is a GaAs layer that contained three planes of Be dopants. The As clusters are seen to coarsen preferentially between the planes of Be dopants. The final top GaAs layer contained a plane of In. There is no apparent effect on the As cluster formation due to the plane of In atoms.

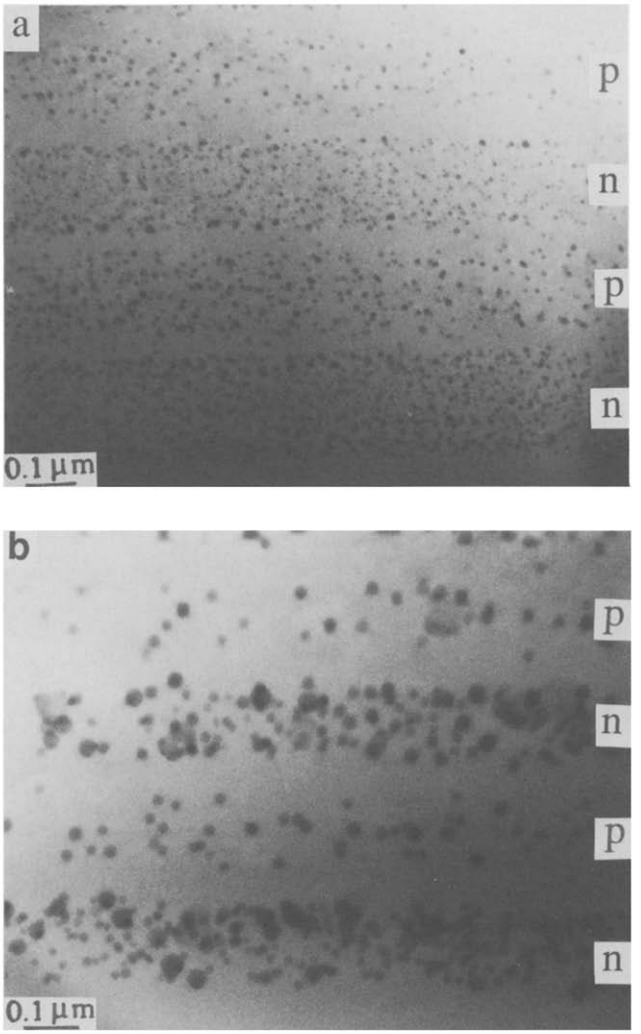

Fig. 5. TEM image of a series of 200 nm GaAs regions uniformly doped with Si at 1×10^{18} cm^{-3} followed by a 200 nm GaAs region uniformly doped with Be at 1×10^{18} cm^{-3}, and subsequently annealed at (a) 700 °C for 30 s and (b) 950 °C for 30 s.

To investigate further the effect of doping on cluster coarsening, a film structure was grown consisting of 200 nm GaAs regions uniformly doped with Si at 1×10^{18} cm^{-3} followed by 200 nm GaAs regions uniformly doped with Be at 1×10^{18} cm^{-3} [34]. Figure 5(a) is a sample from this film annealed for 30 s at 700 °C, and Fig. 5(b) is a sample that was annealed for 30 s at 950 °C. As the As clusters coarsen, there is a preferential coarsening of the clusters from the p-GaAs to the n-GaAs regions.

The above observations of the effects of doping on the cluster coarsening are due to the Schottky nature of the As clusters. An As cluster in n-GaAs will be negatively charged. Therefore, if the cluster thermally emits an As interstitial (As_i), there will be a coulombic attraction between the cluster and the As_i. An As cluster in p-GaAs will be positively charged and so there will be a coulombic repulsion between the cluster and an As_i. Therefore As clusters will be inherently more stable in n-type GaAs than p-type GaAs. Furthermore, an As cluster will be very unstable in a region where there is an electric field.

There is one more interesting phenomenon observed with the formation of As clusters in the presence of dopants. As-grown at low temperature, heavily n-doped GaAs will still be conducting, since As interstitials and As antisites are deep donors. Therefore As clusters readily form with annealing, since the formation of clusters depletes the semiconductor and drives the Fermi level to mid-gap. In contrast, as-grown at low temperature heavily p-doped material is insulating because the deep donor As interstitials and As antisites compensate the material, so the Fermi level is already at midgap. For a GaAs sample grown at 220 °C and doped with Be at 2×10^{19} cm^{-3} we have found that no As clusters form with annealing. Arsenic cluster formation in such a heavily p-doped sample would quickly lead to p-type conduction, since the As in clusters would be much less effective in compensating this material. The result would be that the Fermi level would move from midgap towards the valence band. This represents an increase in energy, which is not offset by the lowering in energy caused by cluster formation. Hence As clusters will not form in heavily p-doped material.

5. Conclusions

In this paper we have described a new composite material consisting of clusters of the semimetal As in arsenide semiconductor matrices. These composites are formed by incorporating excess As in the semiconductor, which precipitates with annealing. The incorporation of the excess As is accomplished by MBE at low substrate temperatures [1]; however, it has been observed recently that the excess As can be incorporated using ion implantation [36]. We have demonstrated that the cluster densities can be controlled with the coarsening anneal. Furthermore, we have demonstrated that heterojunctions and doping can be used to control the positioning of the As clusters.

Acknowledgment

This work was partially supported by the US Air Force Office of Scientific Research under grant numbers F49620-93-1-0031 and F49620-93-1-0388.

References

1 M. R. Melloch, N. Otsuka, J. M. Woodall, A. C. Warren and J. L. Freeouf, *Appl. Phys. Lett., 57* (1990) 1531.
2 K. Mahalingam, N. Otsuka, M. R. Melloch, J. M. Woodall and A. C. Warren, *J. Vac. Sci. Technol., B9* (1991) 2328.
3 J. M. Woodall, G. D. Pettit, C. L. Chang, N. Otsuka, M. R. Melloch, D. Yan and F. H. Pollak, *Appl. Phys. Lett.*, in press.
4 A. C. Warren, J. M. Woodall, J. L. Freeouf, D. Grischkowsky, D. T. McInturff, M. R. Melloch and N. Otsuka, *Appl. Phys. Lett., 57* (1990) 1331.
5 F. W. Smith, A. R. Calawa, C.-L. Chen, M. J. Mantra and L. J. Mahoney, *IEEE Electron. Dev. Lett., 9* (1988) 77.
6 B. J.-F. Lin, C. P. Kocot, D. E. Mars and R. Jaeger *IEEE Trans. Electron. Dev., 37* (1990) 46.
7 M. R. Melloch, D. C. Miller and B. Das, *Appl. Phys. Lett., 54* (1989) 943.
8 F. W. Smith, H. W. Lee, V. Diadiuk, M. A. Hollis, A. R. Calawa, S. Gupta, M. Frankel, D. R. Dykaar, G. A. Mourou and T. Y. Hsiang, *Appl. Phys. Lett., 54* (1989) 890.
9 S. Gupta, P. K. Battacharya, J. Pamaulapati and G. Mourou, *Appl. Phys. Lett., 57* (1990) 1543.
10 A. C. Warren, N. Katzenellenbogen, D. Grischkowsky, J. M. Woodall, M. R. Melloch and N. Otsuka, *Appl. Phys. Lett., 58* (1991) 1512.
11 D. T. McInturff, J. M. Woodall, A. C. Warren, N. Braslau, G. D. Pettit, P. D. Kirchner and M. R. Melloch, *Appl. Phys. Lett., 60* (1992) 448.
12 D. T. McInturff, J. M. Woodall, A. C. Warren, N. Braslou, G. D. Pettit, P. D. Kirchner and M. R. Melloch, *Appl. Phys. Lett., 62* (1993) 2367.
13 A. C. Warren, J. H. Burroughes, J. M. Woodall, D. T. McInturff, R. T. Hodgson and M. R. Melloch, *IEEE Electron. Dev. Lett., 12* (1991) 527.
14 D. D. Nolte, M. R. Melloch, J. M. Woodall and S. J. Ralph, *Appl. Phys. Lett., 62* (1993) 1356.
15 M. R. Melloch, D. D. Nolte, N. Otsuka, C. L. Chang and J. M. Woodall, *J. Vac. Sci. Technol., B10* (1993) 795.
16 D. D. Nolte, M. R. Melloch, S. E. Ralph and J. M. Woodall, *Appl. Phys. Lett., 61* (1992) 3098.
17 M. Kaminska, E. R. Weber, Z. Liliental-Weber, R. Leon and Z. U. Rek, *J. Vac. Sci. Technol., B7* (1989) 710.
18 R. J. Matyi, M. R. Melloch and J. M. Woodall, *Appl. Phys. Lett., 60* (1992) 2642.
19 Z. Liliental-Weber, W. Swider, K. M. Yu, J Kortright, F. W. Smith and A. R. Calawa, *Appl. Phys. Lett., 58* (1991) 2153.

20 M. R. Melloch, K. Mahalingam, N. Otsuka, J. M. Woodall and A. C. Warren, *J. Cryst. Growth, 111* (1991) 39.
21 R. A. Puechner, D. A. Johnson, K. T. Shiralagi, D. S. Gerber, R. Droopad and G. N. Maracas, *J. Cryst. Growth, 111* (1991) 43.
22 M. O. Manasreh, D. C. Look, K. R. Evans and C. E. Stutz, *Phys. Rev. B, 41* (1990) 10272.
23 Z.-Q. Fang and D. C. Look, *Appl. Phys. Lett., 61* (1992) 1438.
24 M. R. Melloch, N. Otsuka, K. Mahalingam, A. C. Warren, J. M. Woodall and P. D. Kirchner, *Mater. Res. Soc. Proc.*, Vol. 241, Materials Research Society, Pittsburgh, PA, 1992, p. 113.
25 J. P. Ibbetson, J. S. Speck, A. C. Gossard and U. K. Mishra, *Appl. Phys. Lett., 62* (1993) 2209.
26 A. C. Warren, J. M. Woodall, P. D. Kirchner, X. Yin, F. Pollak, M. R. Melloch, N. Otsuka and K. Mahalingam, *Phys. Rev. B, 46* (1992) 4617.
27 S. A. McQuaid, R. C. Newman, M. K. Missous and S. O'Hagan, *Appl. Phys. Lett., 61* (1992) 3008.
28 K. Mahalingam, N. Otsuka, M. R. Melloch, J. M. Woodall and A. C. Warren, *J. Vac. Sci. Technol., B10* (1992) 812.
29 K. Mahalingam, N. Otsuka, M. R. Melloch and J. M. Woodall, *Appl. Phys. Lett., 60* (1992) 3253.
30 M. R. Melloch, C. L. Chang, N. Otsuka, K. Mahalingam, J. M. Woodall and P. D. Kirchner, *J. Cryst. Growth, 127* (1993) 499.
31 Y. Horikoshi, M. Kawashima and H. Yamaguchi, *Jpn. J. Appl. Phys., 25* (1986) L868.
32 L.-W. Yin, Y. Hwang, J. H. Lee, R. M. Kolbas, R. J. Trew and U. K. Mishra, *IEEE Electron. Dev. Lett., 11* (1990) 561.
33 M. R. Melloch, N. Otsuka, K. Mahalingam, C. L. Chang, P. D. Kirchner, J. M. Woodall and A. C. Warren, *Appl. Phys. Lett., 61* (1992) 177.
34 M. R. Melloch, N. Otsuka, K. Mahalingam, C. L. Chang, J. M. Woodall, D. Pettit, P. D. Kirchner, F. Cardone, A. C. Warren and D. D. Nolte, *J. Appl. Phys., 72* (1992) 3509.
35 J. P. Ibbetson, J. S. Speck, A. C. Gossard and U. K. Mishra, *Appl. Phys. Lett., 62* (1993) 169.
36 A. Claverie, F. Namavar and Z. Liliental-Weber, *Appl. Phys. Lett., 62* (1993) 1271.